

Quantum State Transfer in Coupled Cavity Arrays with Defects

Jack Mucciaccio¹ and Richard T. Scalettar²

¹*Department of Physics, Coe College, Cedar Rapids, IA 52402, USA*

²*Department of Physics, University of California, Davis, CA 95616, USA*

(Dated: September 11, 2021)

Quantum state transfer (QST) through coupled cavity arrays (CCAs) has become a popular research topic. Recently, it was discovered that perfect QST could be achieved by tuning the parameters of a CCA. We investigated the effect of defects and emitters on the performance of CCAs that have been tuned for perfect QST. Data was generated with the Tavis-Cummings-Hubbard model and t-dependent perfect diagonalization. We find that single defects localize eigenvectors and create traps for photons. We also find that both disorder in a CCA's parameters as well as inserting emitters ruins the perfect QST for a tuned CCA.

I. INTRODUCTION

Quantum state transfer (QST) involves moving a quantum state from some location A to another location B [1, 2]. QST is difficult to achieve since quantum particles typically like to spread their wave functions spatially instead of localizing them at points. To force a wave function to travel between two points, special devices must be engineered which manipulate the wave function in just the right way [1–3]. Improving QST is an important goal of quantum information processing research [1, 2, 4]. Quantum computers will not be possible until a reliable method of QST has been developed [1, 2]. Many QST methods are under development, including optical photons, phonon modes for trapped ions, and spin chains [3, 5]. Recently, QST through coupled cavity arrays (CCAs) has shown significant promise [6].

A CCA is an array of optical cavities which have been placed in a dielectric material like silicon and are coupled through waveguides [3, 6, 7]. Photons can be trapped in these cavities and hop between adjacent cavities. A method for perfect QST in CCAs of any length has already been discovered [3, 7]. In addition, these cavities can contain two level systems known as emitters. These emitters can absorb a photon and then re-emit it. An emitter can only absorb one photon at a time, which gives rise to the photon blockade effect. CCAs are founded in cavity quantum electrodynamics, but they have also become an important topic of research in condensed matter physics [3, 6].

When a photon is in a CCA, its wave function can spread out between the cavities. The use of emitters in CCAs allows for the wave function to spread into the emitters too. When a photon has its wave function split between the cavities and the emitters, it is known as a polariton. Polaritons can be treated as a quasi-particle with interesting properties [4, 7]. While atoms are normally used as the emitters, more exotic two level systems like quantum dots and color centers can also be used [4, 6].

Photons can escape a cavity in the real world, reducing the efficiency of CCAs. However, techniques for constructing optical cavities are improving and modern techniques allow for High Q-factor cavities that are more ef-

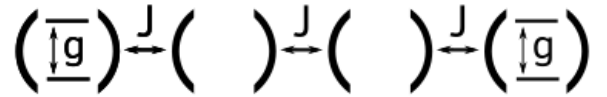


FIG. 1. A diagram of a CCA with four cavities and two emitters. The first emitter is in the first cavity, the second emitter is in the fourth cavity.

ficient [5, 6]. Techniques for constructing wave guides, quantum dots, and color centers have also improved. These improvements should make CCAs significantly easier to produce in the future [3, 4, 6].

II. METHODS

In order to understand the impact of defects and disorder on QST, we performed simulations using the Tavis-Cummings-Hubbard model and perfect diagonalization. Data was generated for the eigenvalues, eigenvectors, and time evolution of the system.

Generating the data was done in four steps:

1. Specify the parameters of the system.
2. Construct the Hamiltonian.
3. Diagonalize the Hamiltonian.
4. Calculate the time evolution of the system.

A. Specifying the Parameters of the System

An example of a simple CCA is shown in Figure 1. Each cavity has an energy E_c and a coupling rate J with any neighboring cavities. Each emitter has an energy E_e and a coupling rate g with the cavity it is located in. For a system with N_c cavities and N_e emitters, there are N_p

parameters with N_p given by (1).

$$N_p = \begin{cases} 1 + 3N_e & N_c = 1 \\ 2N_c + 3N_e & N_c \geq 1 \end{cases} \quad (1)$$

Each emitter contributes an extra parameter because the location of the emitter must be specified.

A defect is represented by a shift in a parameter from its normal value. For example, a cavity energy defect in the N^{th} cavity would be represented by $E_c^N \rightarrow E_c^{N'}$. Disorder is represented by randomized defects across many parameters. For example, cavity energy disorder would give a randomized defect to each cavity energy.

B. Constructing the Hamiltonian

The Tavis-Cummings-Hubbard model was used. The Hamiltonian for this model is given by (2)

$$H = -J \sum_n (a_{n+1}^\dagger a_n + a_n^\dagger a_{n+1}) + \sum_n \left[E_c a_n^\dagger a_{n+1} + \sum_e (E_e \sigma_n^\dagger \sigma_n + g (\sigma_n^\dagger a_n + a_n^\dagger \sigma_n)) \right] \quad (2)$$

where n indexes the cavities and e indexes the emitters. The operators a_n^\dagger and σ_n^\dagger represent the creation of a photon in a cavity and the excitement of an emitter, respectively. The operators a_n and σ_n represent the destruction of a photon in a cavity and the de-excitement of an emitter, respectively.

Only systems with one excitement (one photon) were considered. This simplified the basis to be $N = N_c + N_e$ dimensional. The basis states are $|100\dots 0\rangle$, $|010\dots 0\rangle$, \dots , $|000\dots 1\rangle$. Here, the i^{th} state represents a photon in the i^{th} cavity for $1 \leq i \leq N_c$. For $N_c + 1 \leq i \leq N$, the i^{th} state represents an excitement in the $(i - N_c)^{\text{th}}$ emitter. For example, a system with two cavities and two emitters has the basis states as given in (3).

$$\begin{aligned} |1000\rangle &\leftrightarrow \text{photon in the first cavity} \\ |0100\rangle &\leftrightarrow \text{photon in the second cavity} \\ |0010\rangle &\leftrightarrow \text{first emitter excited} \\ |0001\rangle &\leftrightarrow \text{second emitter excited} \end{aligned} \quad (3)$$

Combining the formula for the Hamiltonian with the basis states as defined above allows us to construct a matrix representation of the Hamiltonian. The Hamiltonian matrix for a system with no emitters has the general form of

$$H = \begin{bmatrix} E_c^1 & J_1 & 0 & \dots & 0 \\ J_1 & E_c^2 & J_2 & \dots & 0 \\ 0 & J_2 & E_c^3 & \dots & 0 \\ \vdots & \vdots & \vdots & \ddots & J_{N_c-1} \\ 0 & 0 & 0 & J_{N_c-1} & E_c^{N_c-1} \end{bmatrix}$$

which is an $N_c \times N_c$ matrix.

For a system with emitters, the Hamiltonian is an $N \times N$ matrix with the top left corner as above. The i^{th} emitter will have E_e^i placed in the position $(i + N_c, i + N_c)$ and will have g_i placed in the positions $(k_i, i + N_c)$ and $(i + N_c, k_i)$. Here, k_i is the index of the cavity that the i^{th} emitter is placed in. For a system with 4 cavities and 2 emitters with the 1st and 2nd emitters in the 1st and 4th cavities, respectively, the Hamiltonian is

$$H = \begin{bmatrix} E_c^1 & J_1 & 0 & 0 & g_1 & 0 \\ J_1 & E_c^2 & J_2 & 0 & 0 & 0 \\ 0 & J_2 & E_c^3 & J_3 & 0 & 0 \\ 0 & 0 & J_3 & E_c^4 & 0 & g_2 \\ g_1 & 0 & 0 & 0 & E_e^1 & 0 \\ 0 & 0 & 0 & g_2 & 0 & E_e^2 \end{bmatrix}.$$

For the same system but with the 1st and 2nd emitters in the 2nd and 3rd cavities, respectively, the Hamiltonian is

$$H = \begin{bmatrix} E_c^1 & J_1 & 0 & 0 & 0 & 0 \\ J_1 & E_c^2 & J_2 & 0 & g_1 & 0 \\ 0 & J_2 & E_c^3 & J_3 & 0 & g_2 \\ 0 & 0 & J_3 & E_c^4 & 0 & 0 \\ 0 & g_1 & 0 & 0 & E_e^1 & 0 \\ 0 & 0 & g_2 & 0 & 0 & E_e^2 \end{bmatrix}.$$

The construction of the Hamiltonian was automated by a C program.

C. Exact Diagonalization

Exact Diagonalization involves numerically solving for the eigenvectors and eigenvalues of the Hamiltonian matrix. If we let $|\psi\rangle$ represent the state of our system, then (4) is the time-independent Schrödinger equation.

$$H |\psi\rangle = E |\psi\rangle \quad (4)$$

Thus the eigenvectors of our system are the stationary states and the eigenvalue corresponding to an eigenvector represents the energy of that eigenvector.

The eigenvectors may be represented by the $N \times N$ matrix S where the i^{th} column of S is the i^{th} eigenvector.

$$S = [\psi_1 \ \psi_2 \ \psi_3 \ \dots \ \psi_N] \quad (5)$$

The eigenvalues may be represented by the diagonal $N \times N$ matrix D , where the i^{th} value on the diagonal is the eigenvalue corresponding to the i^{th} eigenvector.

$$D = \begin{bmatrix} \lambda_1 & 0 & \dots & 0 \\ 0 & \lambda_2 & \dots & 0 \\ \vdots & \vdots & \ddots & 0 \\ 0 & 0 & 0 & \lambda_N \end{bmatrix} \quad (6)$$

D. Time Evolution of the System

The time evolution of a system with initial state $|\psi(0)\rangle$ is given by (7) where we take $\hbar = 1$.

$$|\psi(t)\rangle = e^{-iHt} \cdot |\psi(0)\rangle \quad (7)$$

Here, e^{-iHt} is the exponential of a matrix and is given by (8).

$$e^{-iHt} = \sum_{k=0}^{\infty} \frac{1}{k!} (-iHt)^k = \sum_{k=0}^{\infty} \frac{(-i)^k t^k}{k!} H^k \quad (8)$$

Equation (8) is lengthy to compute due to the repeated matrix multiplications. However using the substitution $e^{-iHt} = S e^{-iDt} S^T$, (8) becomes

$$e^{-iHt} = S \left[\sum_{k=0}^{\infty} \frac{(-i)^k t^k}{k!} D^k \right] S^T \quad (9)$$

where

$$D^k = \begin{bmatrix} \lambda_1^k & 0 & \dots & 0 \\ 0 & \lambda_2^k & \dots & 0 \\ \vdots & \vdots & \ddots & \vdots \\ 0 & 0 & 0 & \lambda_N^k \end{bmatrix} \quad (10)$$

so

$$e^{-iHt} = S \begin{bmatrix} e^{-i\lambda_1 t} & 0 & \dots & 0 \\ 0 & e^{-i\lambda_2 t} & \dots & 0 \\ \vdots & \vdots & \ddots & \vdots \\ 0 & 0 & 0 & e^{-i\lambda_N t} \end{bmatrix} S^T. \quad (11)$$

Compared to (8), (11) is much faster to compute due to the matrix multiplication being replaced by complex exponentials. So the time evolution was calculated as (12).

$$|\psi(t)\rangle = [S e^{-iDt} S^T] \cdot |\psi(0)\rangle \quad (12)$$

This was also implemented in a C program.

The exact diagonalization and the time evolution could both be computed very quickly for systems under consideration. The computations took less than ten minutes for the largest time evolution systems considered here ($N = 512$ and 200 time steps). The fast computation time is due to the nearly tridiagonal shape of the Hamiltonian. A linear algebra system can optimize the computations when so many of the Hamiltonian entries are zero.

E. Perfect QST

It was mentioned earlier that J values for perfect QST in a cavity only system have already been discovered.

For a system with N_c cavities, these perfect J values are given by (13).

$$J_i = \sqrt{i[N_c - (i + 1)]} \quad (13)$$

For a system with 7 cavities, the J values are as shown in (14).

$$J_N = \sqrt{1 \cdot 6} \quad \sqrt{2 \cdot 5} \quad \sqrt{3 \cdot 4} \quad \sqrt{4 \cdot 3} \quad \sqrt{5 \cdot 2} \quad \sqrt{6 \cdot 1} \\ \boxed{1} - \boxed{2} - \boxed{3} - \boxed{4} - \boxed{5} - \boxed{6} - \boxed{7} \quad (14)$$

III. RESULTS

Three types of systems were explored:

1. Cavity only systems with a single defect.
2. Cavity only systems with cavity energy disorder.
3. Cavity systems with a single emitter.

A. Cavity only systems with a single defect

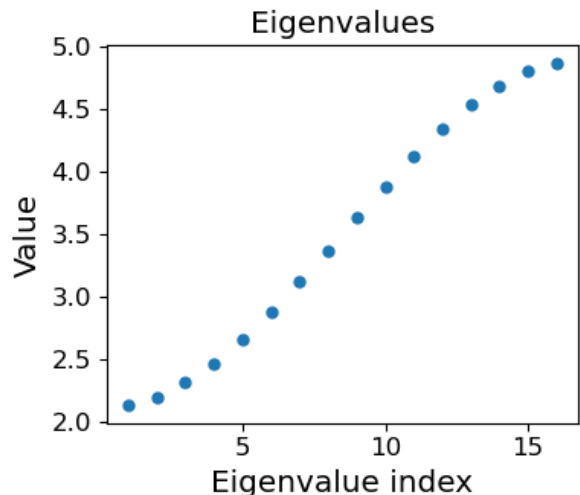


FIG. 2. Eigenvalues in order of magnitude. There are no emitters and no defects in this system. The eigenvalues follow the equation given in (15). Parameters: $N = 16$, $E_c = 3.5$, $J = 0.7$.

This first system will have its eigenvalues and eigenvectors studied instead of its time evolution. The goal is to find the effect that a cavity energy defect will have on the eigenvalues and eigenvectors. Uniform J values and cavity energies are used, $N = 16$, and there are no emitters.

The eigenspectrum for a system with no defect is shown in Figure 2. These eigenvalues are given by (15).

$$E(n) = E_c - 2J \cos\left(\frac{\pi n}{N}\right) \quad \text{where } 0 \leq n < N \quad (15)$$

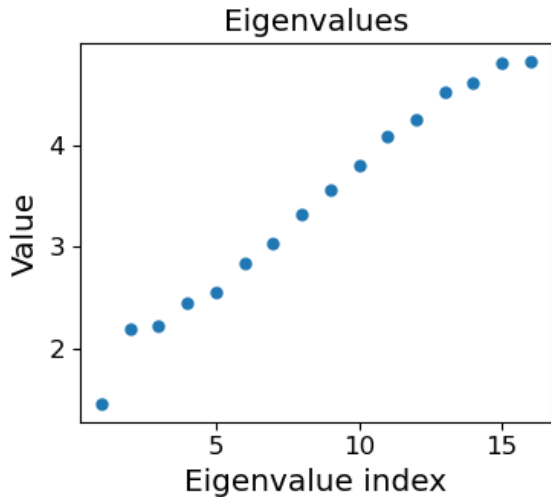


FIG. 3. Eigenvalues in order of magnitude. There are no emitters in this system. There is a defect in the fourth cavity. These eigenvalues are approximate to, but are not equal to, the values from (15). Parameters: $N = 16$, $E_c = 3.5$, $J = 0.7$, $E_c^4 = 2.0$.

The eigenvalues will be in the range $[E_c - 2J, E_c + 2J]$, which for the system in Figure 2 is $[2.1, 4.9)$. Due to the shape of the distribution given by (15), these values are not uniformly distributed in this range. The density of eigenvalues will be higher at the edges of the range than at the center of the range.

The eigenspectrum for a system with a defect in the eighth cavity is shown in Figure 3. The defect shifts all of the eigenvalues while still keeping the general shape of the eigenspectrum from Figure 2. The most affected eigenvalue in Figure 3 is the smallest one, which becomes an outlier far below the range of $[2.1, 4.9)$ from Figure 2.

To analyze the effect of this outlier eigenvalue ψ_1 , Figure 4 and Figure 5 show the probability distribution for ψ_1 with no defect and with a defect, respectively. Figure 4 shows a relatively wide distribution while Figure 5 shows a relatively narrow distribution that is localized around the defective eighth cavity. To quantify the width of these distributions, we define the localization length ζ to be equal to the FWHM (full width at half maximum) of the probability distribution.

Next, we would like to find the relationship between defect magnitude and localization length. We define dE as $dE = E_c - E'_c$ where E_c is the normal cavity energy and E'_c is the defective cavity energy. We assume that the relationship between defect magnitude and localization length is a power law as shown in (16).

$$\zeta \propto dE^p \quad (16)$$

Taking the natural log of both sides of (16) yields (17), which is a linear fit for p in terms of $\ln(\zeta)$ and $\ln(dE)$.

$$\ln(\zeta) \propto p \ln(dE) \quad (17)$$

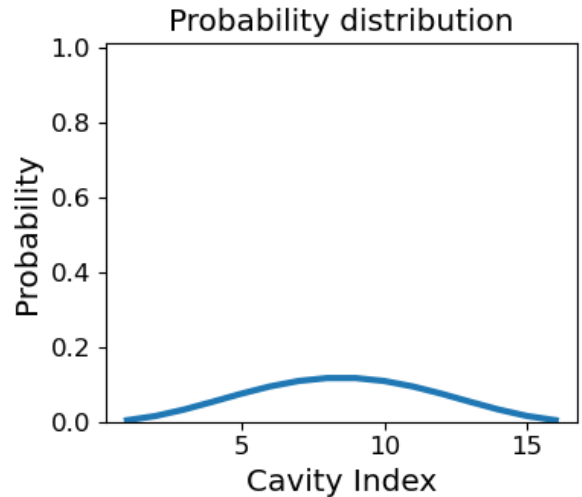


FIG. 4. The probability vs cavity index for the eigenvector ψ_1 corresponding to the lowest energy eigenvalue. The probability is calculated as $|\psi_1|^2$. There are no emitters and no defects in this system. Parameters: $N = 16$, $E_c = 3.5$, $J = 0.7$.

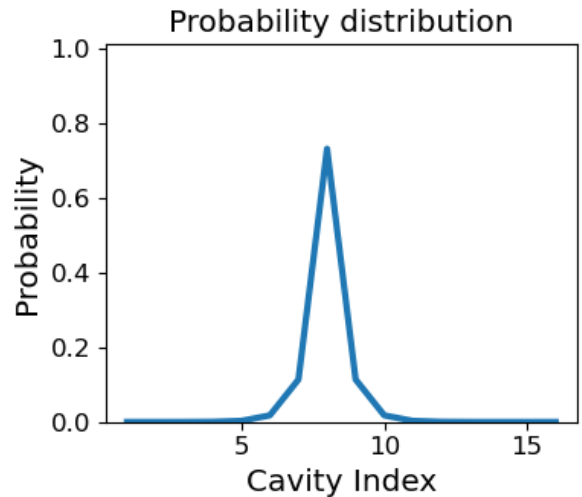


FIG. 5. The probability vs cavity index for the eigenvector ψ_1 corresponding to the lowest energy eigenvalue. The probability is calculated as $|\psi_1|^2$. There are no emitters. There is a defect in the fourth cavity. Parameters: $N = 16$, $E_c = 3.5$, $J = 0.7$, $E_c^4 = 2.0$.

Figure 6 displays data for $\ln(\zeta)$ vs $\ln(dE)$ and contains a curve fit to find the value for p . The curve fit is done for only part of the graph because the relationship between $\ln(\zeta)$ and $\ln(dE)$ breaks down for large dE . Notice that an excitement's position cannot be specified beyond what cavity it is in. The narrowest probability distribution possible is a spike with a probability of 1 in one cavity and a probability of 0 in all other cavities. The FWHM of this distribution is 0.5 and thus $\zeta \geq 0.5$ always. So as

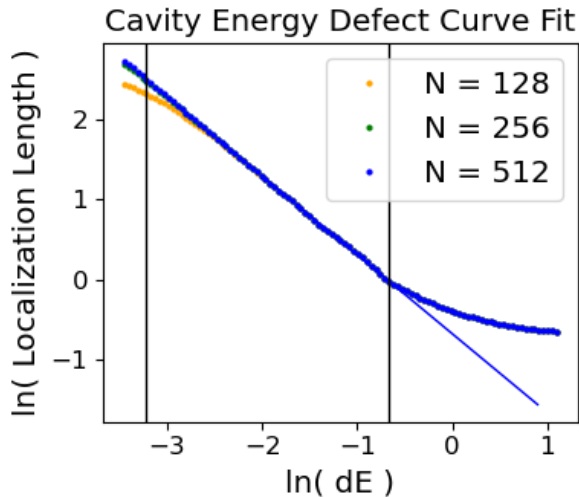


FIG. 6. The probability vs cavity index for the eigenvector ψ_1 corresponding to the lowest energy eigenvalue. The probability is calculated as $|\psi_1|^2$. There are no emitters. There is a defect in the fourth cavity. Parameters: $N = 16$, $E_c = 3.5$, $J = 0.7$, $E_c^4 = 2.0$.

$$\ln(dE) \rightarrow \infty, \ln(\zeta) \rightarrow \ln(0.5) \approx -0.693.$$

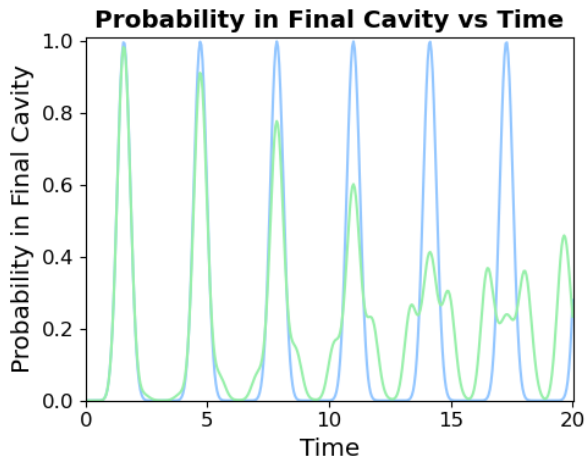


FIG. 7. The probability in the final cavity vs time for the excitation. The blue curve is a system with $\delta = 0$ and the green curve is a system with $\delta = 1$. The probability is calculated as $|\psi|^2$. There are no emitters and the J values are perfect. Parameters: $N = 8$, $E_c^{\text{base}} = 1$.

The curve fit from Figure 6 gives $p = -1$, thus (16) becomes (18).

$$\zeta \propto \frac{1}{dE} \quad (18)$$

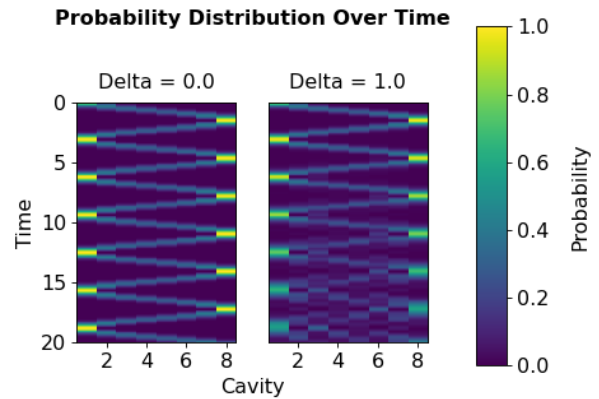


FIG. 8. A heatmap of time vs cavity index where the color represents the probability of the excitation in that cavity. The left heatmap represents a system with $\delta = 0$ and the right heatmap is a system with $\delta = 1$. The probability is calculated as $|\psi|^2$. There are no emitters and the J values are perfect. Parameters: $N = 8$, $E_c^{\text{base}} = 1$.

B. Cavity only systems with cavity energy disorder

We define disorder to mean many randomized defects instead of a single defect. In the case of cavity energy, this means the cavity energies are defined according to $E_c^i = E_c^{\text{base}} + \delta \cdot r$ where $-\frac{1}{2} \leq r \leq \frac{1}{2}$ is an evenly distributed random number. This way every single cavity energy is defective, something that corresponds to real world conditions.

Figure 7 shows the probability in the final cavity vs time for a system with disorder and a system without disorder. These systems have $N = 8$, $E_c^{\text{base}} = 1$ and perfect J values. Since perfect J values are used, the system without disorder displays perfect quantum state transfer. This can be seen in Figure 7 since the system without disorder periodically reaches a probability of 1 in the final cavity. This represents the photon bouncing back and forth between the first cavity and last cavity with no loss in peak height.

For the system in Figure 7 with disorder, the peaks are not periodic. The first few peaks show a rapid decrease in magnitude. The peak shapes begin to deform and secondary peaks are created. The first peak, which represents the fidelity of quantum state transfer, has a probability less than 1. This means the disorder has ruined perfect QST.

Figure 8 contains heatmaps for a system with disorder and a system without disorder. The heatmaps display time vs cavity position with the color representing the probability of a photon. These systems have $N = 8$, $E_c^{\text{base}} = 1$ and perfect J values. Once again, the system with no disorder displays perfect quantum state transfer. The photon appears to travel as a single localized packet, leaving a thin trail on the heatmap. The system with disorder begins with similar behavior. However, the photon's path becomes blurrier as time goes on. The photon

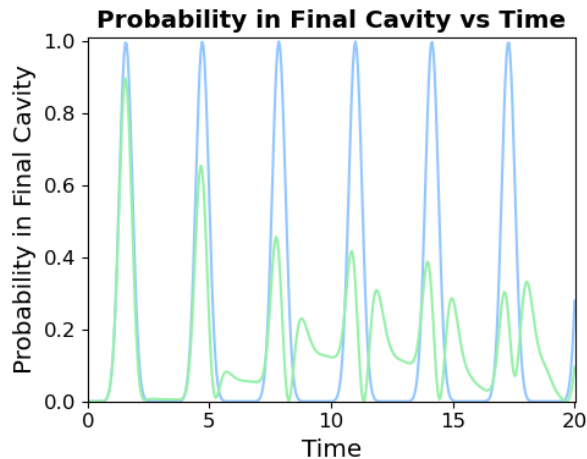


FIG. 9. The probability in the final cavity vs time for the excitement. The blue curve is a system with $\delta = 0$ and the green curve is a system with $\delta = 1$. The probability is calculated as $|\psi|^2$. There are no emitters and the J values are perfect. Parameters: $N = 8$, $E_c^{\text{base}} = 1$.

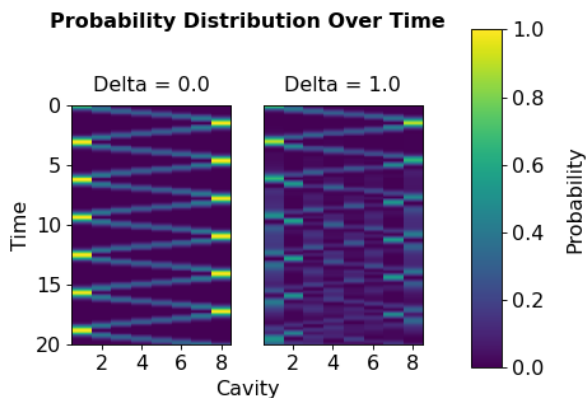


FIG. 10. A heatmap of time vs cavity index where the color represents the probability of the excitement in that cavity. The left heatmap represents a system with $\delta = 0$ and the right heatmap is a system with $\delta = 1$. The probability is calculated as $|\psi|^2$. There are no emitters and the J values are perfect. Parameters: $N = 8$, $E_c^{\text{base}} = 1$.

is spreading out and is no longer traveling as a localized packet.

C. Cavity systems with a single emitter

Figure 9 shows the probability in the final cavity vs time for a system with an emitter and a system without

an emitter. These systems have $N = 8$, $E_c = 1$, $E_e = 1$, $g = 1$, and perfect J values. Since perfect J values are used, the system without an emitter displays perfect quantum state transfer. The photon always returns to the final cavity with a probability of 1.

For the system in Figure 9 with an emitter, the probability in the final cavity peaks at regular intervals, but the first few peaks rapidly decrease in magnitude. Secondary peaks begin to form and the peak shapes are distorted over time. The fidelity is less than 1. So the emitter ruins the perfect QST and modifies the shapes of the peaks. This is a very similar result to the system with disorder in Figure 7.

Figure 10 contains heatmaps for a system with an emitter and a system without an emitter. The heatmaps display time vs cavity position with the color representing the probability of a photon. These systems have $N = 8$, $E_c = 1$, $E_e = 1$, $g = 1$, and perfect J values. The system with no disorder displays perfect quantum state transfer. Notice the stark color contrast between where the photon is and where the photon isn't. However, the system with disorder becomes blurrier as time increases. This means that there is no longer a sharp divide between where the photon is and the photon isn't. The probability of the photon being found in the final cavity drops rapidly. This result is very similar to the system with disorder from Figure 8.

IV. CONCLUSION

Quantum state transfer is a vital part of the roadmap to quantum computers. An important result has shown that CCAs are capable of supporting perfect QST if their parameters are properly tuned. We investigated the effect of defects and emitters on such these CCAs. Data was generated using the Tavis-Cummings-Hubbard model and t-dependent perfect diagonalization. We showed that single defects localized the lowest energy eigenvector and we found a relationship between localization length and defect magnitude. It was also demonstrated that adding disorder to the parameters or adding an emitter ruins the perfect QST of a tuned CCA. The effect on the data of adding disorder and adding an emitter were very similar.

[1] D. P. DiVincenzo, The physical implementation of quantum computation, *Fortschritte der Physik* **48**, 771 (2000).

[2] J. I. Cirac, Z. P. H. J. Kimble, and M. H, Quantum state transfer and entanglement distribution among dis-

- tant nodes in a quantum network, *Physical Review Letters* **78**, 3221 (1997).
- [3] G. M. Almeida, F. Ciccarello, T. J. Apollaro, and A. M. Souza, Quantum-state transfer in staggered coupled-cavity arrays, *Physical Review A* **93**, 032310 (2016).
- [4] S. Bose, D. G. Angelakis, and D. Burgarth, Transfer of a polaritonic qubit through a coupled cavity array, *Journal of Modern Optics* **54**, 2307 (2007).
- [5] M. J. Hartmann, F. G. S. L. Brandao, and M. B. Plenio, Quantum many-body phenomena in coupled cavity arrays, *Laser & Photonics Reviews* **2**, 527 (2016).
- [6] K. J. Vahala, Optical microcavities, *Nature* **424**, 839–846 (2003).
- [7] M. Christandl, N. Datta, T. C. Dorlas, A. Ekert, A. Kay, and A. J. Landahl, Perfect transfer of arbitrary states in quantum spin networks, *Physical Review A* **71**, 032312 (2005).